ORGANOMETALLICS
Article
pubs.acs.org/Organometallics

Synthesis of 2,5-Substituted Siloles and Optical Study of Interactions with Mercury(II), Copper(II), and Nickel(II) Cations

James B. Carroll and Janet Braddock-Wilking*

Department of Chemistry and Biochemistry and Center for Nanoscience, University of Missouri St Louis, St. Louis, Missouri 63121, United States

S Supporting Information

ABSTRACT: Several 2,5-diaryl-1,1-dimethyl-3,4-diphenylsiloles (with aryl = *p*-cyanophenyl (**1**), *m*,*p*-bis(methylthio)phenyl (**2**), *p*-*N*,*N*-dimethylaminophenyl (**3**), 2,2′-bipyridin-6-yl (**4**)) were synthesized and characterized by UV−vis, fluorescence, and NMR spectroscopy, along with crystal structure determinations for **1** and **2**. Compounds **1**−**4** in methylene chloride were combined with 1−10 equiv of M(ClO_4)$_2$ (M = Ni, Cu, Hg) in methanol, and the resulting solutions were monitored by UV−vis and fluorescence spectroscopy. Compound **1** showed slight effects for each metal, **2** exhibited fluorescence quenching selectively for Hg(II), **3** showed significant changes for all cations, and **4** generally demonstrated fluorescence quenching for all cations. A discussion of the causes behind these changes is also presented.

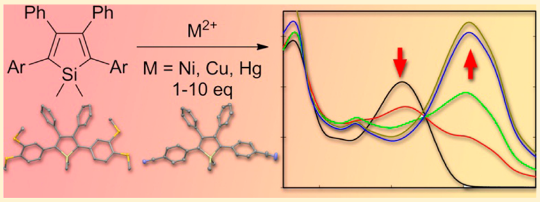

■ INTRODUCTION

Siloles, or 1-silacyclopentadienes, and systems containing the silole motif continue to receive appreciable interest. In comparison to analogous cyclopentadienes, siloles exhibit red-shifted absorption and emission spectra and greatly increased electron mobility[1] and affinity;[2] these differences are attributed to a lowered LUMO energy due to overlap of the σ^* and π^* orbitals from the silylene and butadiene fragments, respectively.[3] Further, the observed physical and electronic effects can be greatly influenced by the substituents chosen. The degree of radiative relaxation in the solution and solid states can be controlled through judicious selection of moderately and significantly bulky substituents,[4] which can greatly affect the observed quantum yield.[5] Though physical effects can be manipulated at all positions along the silole ring, the most significant contributions to electronic properties (e.g., absorption and emission maxima) come from the substituents at the 2,5-positions.[6] Both strong π-donors and acceptors on aryl substituents at these sites can induce substantial bathochromic shifts, and asymmetric siloles have been synthesized to take advantage of these donor and acceptor substituents in concert.[7] Because of these varied avenues for manipulation of the desired optoelectronic properties, siloles and related molecules have been studied as components in diverse applications such as organic field-effect transistors (OFETs),[8] organic light-emitting diodes,[9] photovoltaics,[10] and sensors.[11]

Because of the rich electronic variations that siloles present, we desired to investigate several changes in optoelectronic properties upon interaction with metal ions. A significant amount of substituents that affect the properties of the silole can also be envisioned to have some coordinating ability to metal ions. Appreciable changes in properties can then be explored for potential chemosensor applications. Though covalent coordination of metal centers directly to the silole ring, in both η^4 and η^5 modes, have been known for many years,[12] coordination of metals at groups bound to the 2,5-positions has been a relatively recent development. Wang and co-workers reported the synthesis of two siloles with nitrogen-containing substituents that could coordinate to zinc,[13] and a short time later Gerbier's group reported one of the same siloles along with optical data on coordination with both zinc and copper;[14] the compound exhibited stark differences in fluorescence depending on the metal center employed. Recently, Tang and co-workers synthesized a terpyridine-substituted silole that showed selective fluorescent enhancement for zinc.[15] Our group has also investigated some phosphine-linked siloles and their optical changes upon coordination to gold and platinum.[16] We report herein the preparation of some known and new siloles chosen for their potential to bind to metal cations, along with optical spectra outlining the differences in the changes observed on the basis of the metal and silole employed. For our initial studies the perchlorate salts of nickel(II), copper(II), and mercury(II) were chosen in order to study the effects of paramagnetic or heavy-atom species. The results of these studies are described herein.

■ RESULTS AND DISCUSSION

Synthesis. Siloles **1**−**4** were prepared using the standard Tamao one-pot reductive cyclization procedure,[17] outlined in Scheme 1. The new siloles **1** and **2**, along with known siloles **3** and **4**, were isolated as yellow powders in moderate yields (39−53%, based on starting silane). The reagent to synthesize **2**, 4-

Received: January 11, 2013
Published: March 1, 2013

dx.doi.org/10.1021/om400022f | *Organometallics* 2013, 32, 1905−1912

Scheme 1

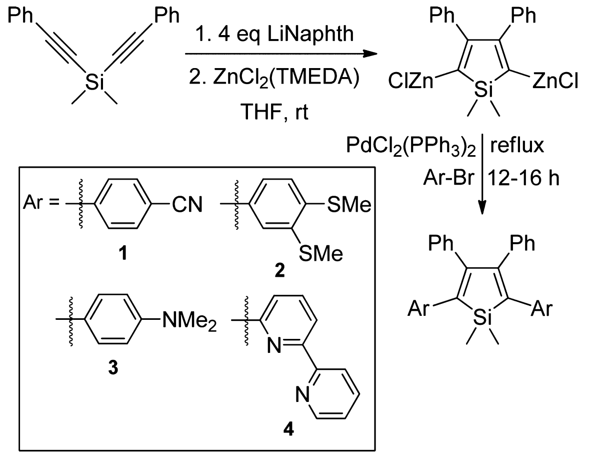

bromo-1,2-bis(methylthio)benzene, was not available commercially and was prepared according to the literature procedure.[18] The new siloles **1** and **2** were characterized by ^{1}H, ^{13}C{^{1}H}, and ^{29}Si{^{1}H} NMR, UV−vis, and fluorescence spectroscopy, elemental analysis, and X-ray crystallography. The known siloles **3**[17b] and **4**[19] were also characterized by ^{1}H and ^{13}C{^{1}H} NMR; the spectra showed good agreement with the literature values. All of the siloles exhibited characteristic NMR shifts, including the ^{13}C{^{1}H} shifts at ca. 152 and −3.0 ppm for the 3,4-silole carbons and methyl carbons attached at the silicon center, respectively. The two new siloles also exhibited ^{29}Si shifts at 9.3 and 7.9 ppm for **1** and **2**, respectively; these values are similar to other reported silole ^{29}Si shifts.[16]

On occasion, after addition of the $ZnCl_2$(TMEDA) to make the intermediate dizinc silole (see Scheme 1), the reaction solution would become viscous and gel-like, at times to the point of preventing stirring. The cause of this gelation could not be fully identified. Subjecting the reaction contents to sonication with a sonicating bath for 10−15 s dispatched the viscous aspect, and the mixture was then able to be stirred to complete the reaction. Curiously, whether this gelation occurred or not did not have a significant impact on the overall yields observed. Rigorous purification of starting materials did not reduce the chances of this phenomenon occurring; however, increasing the time stirred after the addition of the silane (vide infra) from the standard time of 10 min[17b] to at least 30 min prior to addition of $ZnCl_2$(TMEDA) also reduced the chances for gelation considerably. Notably, reactions using lithium without higher sodium content (0.5−1.0%) cause the reductive cyclization to fail, as noted by Morra and Pagenkopf;[20] lithium with added copper stabilizer also seems to give much lower yields.

X-ray Crystal Structures. Crystals of sufficient quality for the new siloles **1** and **2** were grown by slow evaporation and slow diffusion, respectively (see the Experimental Section), as thin needles. Compound **2** refined with three molecules of methylene chloride per molecule of **2**. The structures were solved and refined to reasonable geometries and residual electron densities. Table S-1 in the Supporting Information gives the crystallographic data for compounds **1** and **2**.

The molecular structures of **1** and **2** are shown in Figures 1 and 2, respectively. Compound **1** exhibits a structure that is very similar to that of the unsubsituted phenyl compound 1,1-dimethyl-2,3,4,5-tetraphenylsilole (TPS).[21] Both compounds exhibit the propeller-like arrangement characteristic of 2,3,4,5-tetraphenylsiloles and their analogues.[21] Given that the cyano substituent on the 2,5-phenyl groups is para to the silole ring, the steric influence on the geometry is minimal. The magnitudes of the phenyl torsion angles for **1** at the 2,5-positions are 36.5 and 53.7°, while for TPS they are 34.8 and 48.8°.[21] The torsion angles at the 2,5-positions of **2**, however, are slightly smaller, with a magnitude of 28°. Counter to an assumption that **2** would pack to minimize steric strain, the methylthio substituent meta to the silole ring turns toward the 3,4-phenyl groups. On the basis of steric assumptions alone, this observation is unexpected. The difference Fourier map suggests that the hydrogen atoms on the thiomethyl groups are accurately placed; one of these atoms is oriented toward the centroid of the 3,4-phenyl rings in a manner that suggests some

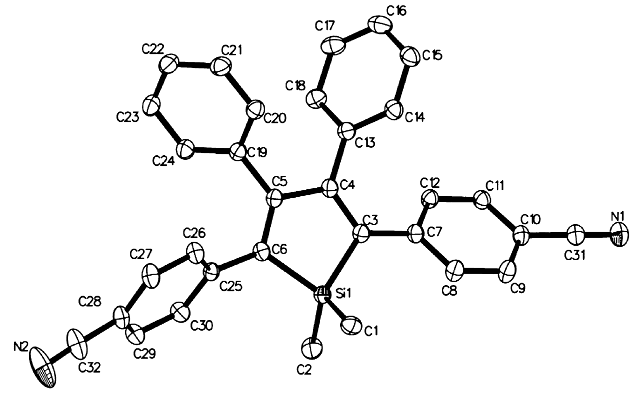

Figure 1. Molecular structure of **1**. Hydrogen atoms have been removed for clarity. Thermal ellipsoids are drawn at the 50% probability level. Selected bond distances (Å), bond angles (deg), and torsion angles (deg) for **1**: Si1−C1 = 1.873(1), Si1−C2 = 1.859(1), Si−C3 = 1.883(1), Si−C6 = 1.880(1), C3−C4 = 1.366(1), C5−C6 = 1.361(1), C31−N2 = 1.146(2), C32−N1 = 1.150(2); C3−Si1−C6 = 91.54(4), C2−Si1−C1 = 110.09(5), C10−C32−N1 = 179.4(1), C28−C31−N2 = 177.3(2); C12−C7−C3−C4 = −36.5(2), C3−C4−C13−C14 = −58.2(1), C6−C5−C19−C24 = −56.5(1), C5−C6−C25−C26 = −53.7(1).

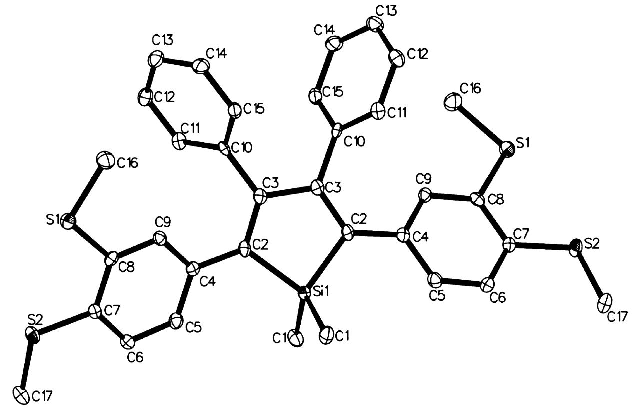

Figure 2. Molecular structure of **2**. Hydrogen atoms and solvent molecules have been removed for clarity. Thermal ellipsoids are drawn at the 50% probability level. Selected bond distances (Å), bond angles (deg), and torsion angles (deg) for **2**: Si1−C1 = 1.873(4), Si1−C2 = 1.887(3), C2−C3 = 1.362(4), C3−C3 = 1.500(5), C8−S1 = 1.768(3), S1−C16 = 1.798(4); C1−Si1−C1 = 108.7(2), C2−Si1−C2 = 92.1(1), Si1−C2−C3 = 107.4(2), C8−S1−C16 = 103.1(2), C7−S2−C17 = 102.4(2); Si1−C2−C4−C5 = −28.0(4), C2−C3−C10−C11 = −64.0(4), C9−C8−S2−C17 = −11.5(3).

possible C−H···π interactions.[22] Compound **2** also has a larger torsional magnitude of the 3,4-phenyl substituents (64.0°) in comparison to **1** (56.5°), perhaps to accommodate for the thiomethyl substituent. These observations, viz., the smaller 2,5-torsional angle and weak intersubstituent interactions, may help explain some of the photometric data recorded for **2** (vide infra).

Electronic Transitions. The UV−visible and fluorescence spectra and quantum yields for the new siloles **1** and **2** were recorded and are given in Table 1. Also given are the optical spectral data for known siloles **3** and **4** along with the literature values.

Table 1. UV−Visible and Fluorescence Spectral Data for the Reported Compounds[a]

compd	λ_{max}, absorbance (nm)	log ε	λ_{max}, fluorescence (nm)	Φ_f, %
1	365	4.12	482	0.25[b]
2	390	4.29	511	1.58[c]
3[d]	415 (423)	4.32 (4.33)	549 (529)	(0.251)
4	382 (386)[e]	3.99	472 (489)[e]	(<0.1)[f]

[a] Spectral data from siloles in a 1/1 CH_2Cl_2/MeOH mixture, 5×10^{-5} M. [b] With reference to 9,10-diphenylanthracene. [c] With reference to fluorescein. [d] Literature values are given in parentheses.[17b] [e] Literature values are given in parentheses.[19] [f] Literature values are given in parentheses.[23]

The optical data of **1** indicate that the cyano substituent has a relatively modest effect on the electronics of the silole; in comparison to TPS,[21] there is a 7 and 12 nm bathochromic shift in the absorbance and fluorescence λ_{max} values, respectively. This corroborates with the very similar structural features of **1** and TPS (vide supra). It appears that the cyano substituent is not suitably positioned to be an effective π-withdrawing group (relative to the 2,5-phenyl moieties); the ability to either be a π donor or acceptor has the most effect on the electronics of siloles.[6] Tang's group used dicyanovinyl substitution, allowing the withdrawing cyano groups to interact more effectively with the π system of the silole; this group affected significant bathochromic shifts relative to the parent silole TPS.[24] The moderate communication of the cyano group in **1** will also be addressed in the metal interaction section (vide infra).

The optical spectra of **2** show further shifts to lower energy in comparison to **1**. In solution, the largest contribution to this observation is likely the modest donating ability of the lone pairs of the sulfurs on the methylthio substituents. The related methoxy substituent, situated para to the silole ring on the 2,5-phenyl groups, induces a bathochromic shift of 12 nm in the absorption λ_{max} in comparison to the methyl analogue for this reason.[17b] Compound **2** also exhibits a significantly higher solution quantum yield. While higher steric hindrance from a methylthio group meta to the silole could help explain this observation,[5] the solid-state arrangement of this substituent, preferring an orientation that suggests some interaction with the 3,4-phenyl groups (Figure 1), could also help explain this increase.

Siloles **3** and **4** both were characterized by UV−vis and fluorescence spectroscopy and agreed reasonably well with the literature values. The slight differences in λ_{max} of the absorbance and fluorescence are most likely from differences in solvent polarity (literature sources used chloroform[17b] for **3** and THF[19] for **4**). Compound **3** exhibits significant bathochromic shifts from TPS due to the strong π-symmetric donating ability of the dimethylamino substituent.[6] Compound **4** exhibits a red shift in the absorbance maximum in comparison to TPS, but a fluorescence blue shift. In the known crystal structure,[23] the torsional angles between the silole core and the adjoining pyridine moieties in **4** are between 26 and 36°, in the approximate range of the silole structures presented herein. Therefore, the extended conjugation brought on by the bipyridine moiety does not significantly affect the electronics of the silole, probably due to its own strong tendencies as a π-accepting unit. The siloles containing 2,5-bis(pyridin-3-yl) and 2,5-bis(pyridin-2-yl) groups[17b] also had a slight bathochromic shift in the absorbance spectra and had little effect on the fluorescence spectrum in comparison to TPS.

Studies with Metal Salts. All of the reported compounds were tested with nickel(II), copper(II), and mercury(II) perchlorate salts. Copper(II) was chosen because of its paramagnetic nature; typically paramagnetic ions cause significant quenching, and we desired to determine to what end this occurred with the siloles reported herein. Nickel(II) also has some known quenching ability,[25] given its ability to form diamagnetic or paramagnetic complexes. Mercury(II) was chosen for several reasons. Being an environmentally harmful ion, the potential for selective and sensitive detection has been a steady area of research.[26] Also, it too is generally seen as an efficient quencher due to the phenomenon known colloquially as the "heavy-atom effect".[27] As shown below, these metal ions have differing abilities to quench (or enhance) fluorescence on the basis of the 2,5-substituent chosen.

Figure 3 shows the results of each silole upon interaction with 10 equiv of the metal ion. For clarity, the absorbance and emission spectra of **3** with the metals were separated. Also tested were 1, 2, and 5 equiv (see Experimental Section), and these spectra are shown in the Supporting Information. During these experiments, the total concentration of silole in the system was kept constant at 5×10^{-5} M, and the volume of silole solution (in methylene chloride) to metal solution (in methanol) was also 2 mL to 2 mL in order to directly compare the changes on using different metals and different equivalencies. Equivalencies of the metal solution were adjusted by changing the concentration of the metal perchlorate in methanol. In order to get an accurate representation of the silole in the absence of metal ion, the spectrum of each silole was measured with 1/1 methylene chloride/methanol to keep the concentration and overall solvent polarity constant.

Compound **1** showed slight changes overall in the optical spectra (Figure 3a). The absorbance λ_{max} upon addition of the metals is essentially unchanged. This suggests that, through the combination of the slight communication of the cyano substituent and the general lability of the group with metal ions, the metal ions studied here do not have significant contributions to the ground state of the silole. The fluorescence spectrum with the metal ions showed variable differences, from none with copper(II) to the most with mercury(II). Interestingly, the fluorescence features are preserved between nickel(II) and mercury(II), and there is no quenching with 10 equiv of copper(II). The slight hypsochromic shift in the fluorescence data along with no discernible changes in the absorbance spectrum might indicate that some excited-state decoordination is occurring,[28] as the changes in the overall electronics of the system for this phenomenon generally reflect the observed data for **1**.

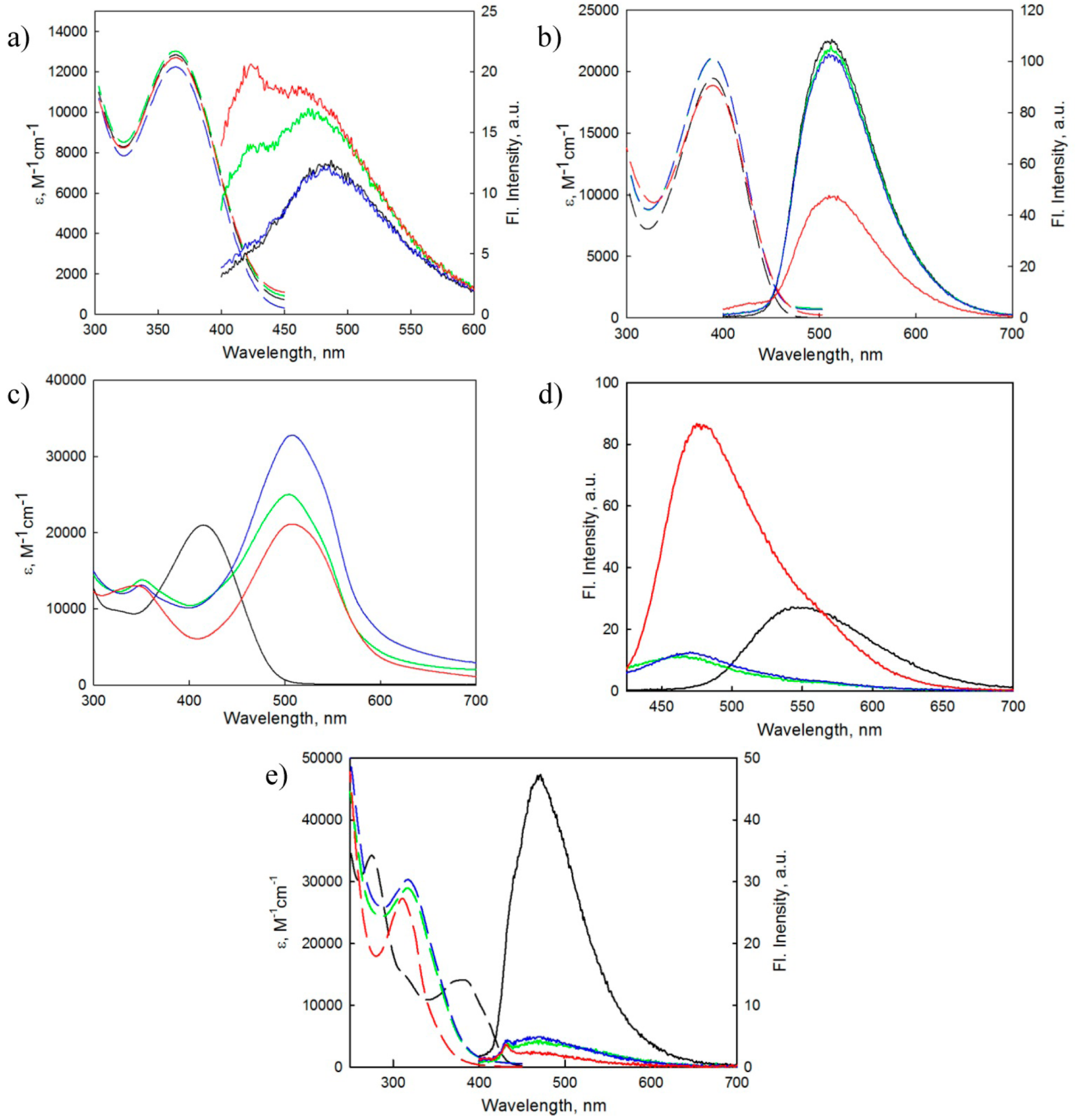

Figure 3. Optical spectra of each of the reported siloles and the mixtures with 10 equiv of the metal perchlorate: (a) UV–vis (dashed) and fluorescence (solid) spectra of **1** with metal solutions; (b) UV–vis (dashed) and fluorescence (solid) spectra of **2** with metal solutions; (c) UV–vis spectra of **3** with metal solutions; (d) fluorescence spectra of **3** with metal solutions; (e) UV–vis (dashed) and fluorescence (solid) spectra of **4** with metal solutions. Legend: (red) mercury(II); (blue) copper(II); (green) nickel(II); (black) pure silole. The wavelengths for fluorescence excitation are 365 nm (**1**), 390 nm (**2**), 415 nm (**3**), and 383 nm (**4**).

Silole **2** was synthesized to affect some selectivity among the metals studied. The absorbance spectrum of **2** also exhibits little change in the presence of the metal ions (Figure 3b), indicating that the metals involved do not change the electronics of the silole core significantly. The fluorescence is unaffected by both nickel(II) and copper(II), but there is significant quenching of the emission from mercury(II). It should be noted that quenching was not appreciable on **2** until 10 equiv of mercury(II) was added (see the Supporting Information). Complexes containing the bis(methylthio)phenyl moiety with mercury ions and compounds are known elsewhere,[29] but the reported spectra here suggest that even binding to mercury on **2** is rather labile. Nevertheless, the selectivity of the methylthio substituents for mercury(II), as predicted by the well-known Pearson acid–base theory (HSAB theory),[30] could make analogues based on **2** a useful template for selective detection of this ion.

Silole **3** has the most significant spectral changes of any in the sample of siloles studied herein. With all metals studied, there is a relatively intense absorption peak ca. 85 nm lower in energy than that for the parent silole (Figure 3c). Notably, a smaller peak ca. 65 nm higher in energy also exists in all cases. The local maxima for the silole with each metal do not vary greatly; this suggests that the new transitions are mainly due to electronic changes in the silole. Figure 4 shows an example of **3** with various amounts of copper. From this plot the two new absorption bands seem to appear at the same time. In a preliminary titration experiment (Figure 5), THF was used for both the silole and metal solutions in order to determine the effects on coordination with a more coordinating solvent. The blue-shifted peak in this experiment appears first, with a relative intensity similar to that before, but the lower energy band appears after much more metal ion solution has been added, at a much lower intensity.

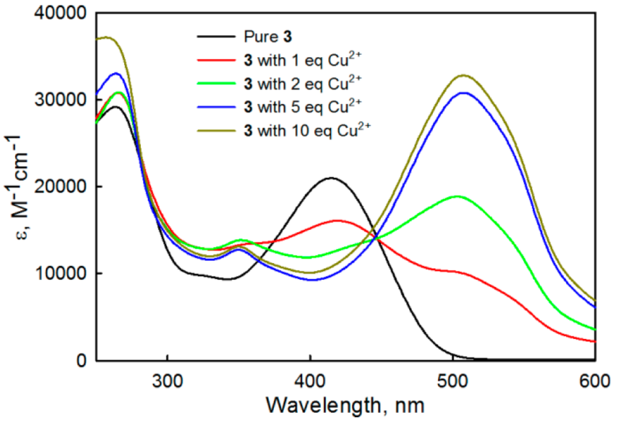

Figure 4. Compound **3** (5×10^{-5} M in methylene chloride) with 1−10 equiv of copper(II) perchlorate solution (in methanol).

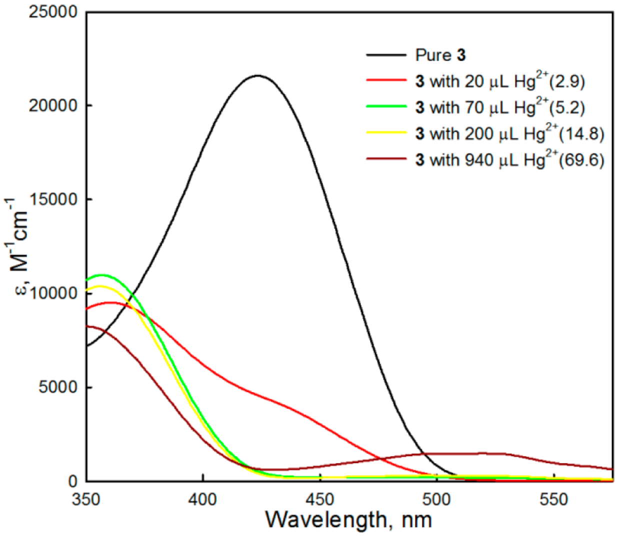

Figure 5. Selected titration data of a solution of **3** in THF (6×10^{-5} M), titrated with 1.3×10^{-2} M mercury(II) perchlorate solution in THF. The values in parentheses in the legend represent the equivalents of mercury(II) in solution.

Hence, the blue-shifted absorption is considerably less dependent on the solvent, but the low-energy band greatly depends on the solvent's coordinating ability. From these data, both bands can be attributed to interaction of **3** with the metal ion. The reduced intensity, higher energy band (compared to **3**) is characteristic of reducing the donating abilities of amino substituents (a photoinduced charge transfer, or PCT, effect);[31] the absorbing peak energy is now much closer to that of TPS, suggesting deactivation of the amino group due to coordination. The increased intensity of the lower energy band in noncoordinating solvents also indicates some manipulation of the PCT effect, but through interaction with the acceptor (i.e., the silole ring) by making the PCT from the amino group to the silole more efficient, thus increasing the absorption coefficient.[31] Given that the silole ring and accompanying aromatics of the "acceptor" region will likely coordinate with ions through arene interactions, the decrease in intensity in THF can be justified, as this coordination mode can be considered more labile than amine coordination and will be much more affected by the competing coordinating ability of the solvent (for a model of the coordination modes, see Figure S-35 in the Supporting Information). Studies on the specific nature of this bonding are ongoing.

The fluorescence spectrum of **3** with the metals is notable in the differences upon changing the ion used. Every metal ion studied induces a similar hypsochromic shift in the fluorescence maximum, suggesting that this change is again due to coordination to, and deactivation of, the amino donating group;[31] this shift to higher energy corresponds to the initial higher energy shift of **3** in THF after addition of metal ion solution (Figure 5). However, the "acceptor-bound" bathochromic shift in the UV−visible spectrum of **3** (Figure 3c) does not seem to have a correlated shift in the fluorescence spectrum; this is possibly due to the nature of the intraligand charge transfer on excitation. While nickel(II) and copper(II) exhibit a lower intensity than **3**, mercury(II) is exceptional in its significant increase in the fluorescence intensity. Part of this difference might be due to self-absorption of the fluorescence by the absorbance band near 500 nm, shown in the UV−visible spectrum (Figure 3c), which is more intense for copper(II) and nickel(II). The increase in intensity on addition of mercury(II) to **3** could be due to oligomeric species, as **3** has two possible coordinating amino subsituents. An increase in the quantum yield on addition of zinc(II) to a terpyridine-substituted silole, reported by Yin et al., was attributed to oligomer formation that would reduce intramolecular rotations and thus decrease the amount of nonradiative decay.[15]

The UV−visible spectrum of **4** (Figure 3e) follows a trend similar to that for the other siloles, in that differences among the metal ions are slight with regard to λ_{max} values. In all cases, a new band appears at ca. 315 nm. Though this band is higher in energy than the silole absorbance at 383 nm, it has a significant increase in intensity, which more closely matches the pure silole peak at 275 nm. Pyridine-based groups are considered stronger π-acceptors than siloles,[15] and therefore this metal-induced shift is likely from the higher energy pure silole band. These factors combined suggest that the metal−silole band is, again, a consequence of the metal binding to the bipyridine moieties (for a model of the coordination see Figure S-35 in the Supporting Information) and making intramolecular PCT more efficient by increasing the accepting ability of those moieties.[31] The fluorescence spectra with each metal show that there is very significant quenching. The UV−visible spectra indicate that the silole band completely disappears, and therefore excitement at the silole peak probably causes a charge transfer to the bipyridine moiety such that fluorescence is attenuated. Bipyridine is a chelating ligand, and so coordination to each ion with **4** is very efficient; the fluorescence quenchings for copper(II) and mercury(II) are very similar even at 2 equiv (see the Supporting Information), with nickel(II) exhibiting less quenching. The exception for nickel(II) is most likely due to its relatively slow ligand exchange kinetics, as ligand exchange of the hexakis(methanol) complex of nickel(II) is approximately 4 orders of magnitude slower than for the copper(II) complex.[32]

In conclusion, two new siloles along with two known siloles were prepared according to the standard Tamao reductive cyclization procedure. The substituents at the 2,5-positions were chosen for the potential to coordinate with metal ions, and the siloles were initially studied for interactions using nickel(II), copper(II), and mercury(II) perchlorate salts. While siloles were affected to various degrees depending on the metal, most changes in the spectra were consistent between metals, but their intensity varied, sometimes significantly. Compound **1** showed slight changes to its fluorescence on addition of the metal perchlorate solutions. Compound **2** differed in that mercury(II) selectively began to quench fluorescence. Compound **3** exhibited significant changes in both the absorption and emission spectra, and intensity of fluorescence differed significantly between the various metal ions. Compound **4** displayed significant quenching with all metal ions studied, and the absorbance suggested that contributions from the silole ring are essentially removed. Studies on the nature of changes observed for these siloles are in progress, along with expanding the metal centers to observe whether the changes observed continue to occur.

■ EXPERIMENTAL SECTION

General Procedures. Reactions were carried out under an argon atmosphere using standard Schlenk techniques with solvents dried and purified by standard methods, unless otherwise notified. The compounds 4-bromo-*N*,*N*-dimethylaniline, 4-bromobenzonitrile, *n*-butyllithium (2.5 M in hexanes), 6-bromo-2,2′-bipyridine, nickel(II) perchlorate hexahydrate, copper(II) perchlorate hexahydrate, and mercury(II) perchlorate hexahydrate were purchased from Aldrich Chemical Co. and used as received. Dichlorodimethylsilane was purchased from Aldrich Chemical Co. and purified by distillation over K_2CO_3 under an inert atmosphere prior to use. Phenylacetylene was purchased from GFS Chemicals, Inc., and used as received. Chloroform-*d* was purchased from Cambridge Isotopes, Inc., and dried over activated sieves prior to use. The following compounds were prepared according to the literature: dimethylbis(phenylethynyl)silane,[20] 1-bromo-3,4-bis(methylthio)benzene,[18] bis(triphenylphosphine)palladium(II) chloride,[33] and zinc(II) chloride−TMEDA.[34] The ^{1}H, $^{13}C\{^{1}H\}$, and $^{29}Si\{^{1}H\}$ NMR (DEPT) spectra were recorded on a Bruker ARX-500 MHz spectrometer in $CDCl_3$. Proton and carbon NMR shifts were referenced internally to residual peaks of the solvent used. Silicon NMR shifts were referenced externally to $SiMe_4$. UV−visible spectra were recorded on a Cary 50 Bio UV−visible spectrometer, and fluorescence spectra were recorded on a Cary Eclipse fluorescence spectrometer. X-ray structural determinations were performed using a Bruker Apex II diffractometer equipped with a CCD area detector. Elemental analyses of the compounds were obtained from Atlantic Microlabs, Inc., Norcross, GA.

Preparation of 2,5-Bis(*p*-cyanophenyl)-1,1-dimethyl-3,4-diphenylphenylsilole (1). Lithium (55 mg, 7.9 mmol), naphthalene (1.1 g, 8.6 mmol), and dry THF (12 mL) were combined and sonicated[20] for 2 h to form a deep green solution of lithium naphthalenide. A solution of dimethylbis(phenylethynyl)silane (0.50 g, 1.9 mmol) in dry THF (8 mL) was added dropwise to the solution over 15 min via an addition funnel. This mixture was stirred for 20 min and cooled to 0 °C. Then, $ZnCl_2$(TMEDA) (2.1 g, 8.3 mmol) was added as a solid at once, followed by additional dry THF (15 mL). If gelation occurred (vide supra), the contents were sonicated for several seconds in a sonicating bath. After the mixture was stirred for 1.5 h, 4-bromobenzonitrile (0.73 g, 4.0 mmol) and $Pd(PPh_3)_2Cl_2$ (60 mg, 0.085 mmol) were successively added, and the mixture was refluxed overnight. The solution was quenched with 1 M HCl. The aqueous layers were combined and extracted with Et_2O (2 × 20 mL), and the organics were combined, washed with water, sodium bicarbonate solution, and brine, and dried with $MgSO_4$. The solvents were removed by rotary evaporation, and the crude mixture was subjected to silica gel column chromatography (hexanes then hexanes/Et_2O, 10/1) to obtain compound **1** as a yellow powder (0.35 g, 40% yield). Mp: 229−230 °C. X-ray-quality crystals were obtained by slow evaporation of an Et_2O solution of **1** at room temperature. ^{1}H NMR (500 MHz): δ 7.43−7.39 (m, 4H, ArH), 7.09−6.98 (m, 10H, ArH), 6.75−6.73 (m, 4H, ArH), 0.48 (s, 6H, SiMe). $^{13}C\{^{1}H\}$ NMR (125 MHz): δ 156.2, 144.9, 141.7, 137.4, 132.1, 129.8, 129.3, 127.9, 127.2, 119.3, 109.3, −4.0. $^{29}Si\{^{1}H\}$ NMR (99 MHz): δ 9.3. Anal. Calcd for $C_{32}H_{24}N_2Si$: C, 82.72; H, 5.21. Found: C, 82.51; H, 5.14.

Preparation of 2,5-Bis[3,4-bis(methylthio)phenyl]-1,1-dimethyl-3,4-diphenylsilole (2). The compound was prepared by a procedure similar to that for compound **1** above except for using 1-bromo-3,4-bis(methylthio)benzene (0.99 g, 4.0 mmol) as the cross-coupling reagent. The material was subjected to silica gel column chromatography (hexanes then hexanes/ethyl acetate, 1/2) to obtain compound **2** as a yellow powder (0.58 g, 51% yield). Mp: 187−189 °C. X-ray-quality crystals were grown from a slow diffusion of methanol into a CH_2Cl_2 solution of **2**. ^{1}H NMR (500 MHz): δ 7.05−7.03 (m, 8H, ArH), 6.86 (dd, *J* = 6.86, 1.85 Hz, 2H, ArH), 6.84−6.81 (m, 4H, ArH), 6.64 (d, *J* = 1.85 Hz, 2H, ArH), 2.44 (s, 6H, SMe), 1.97 (s, 6H, SMe), 0.51 (s, 6H, SiMe). $^{13}C\{^{1}H\}$ NMR (125 MHz): δ 154.4, 140.6, 139.2, 137.4, 137.2, 134.0, 130.1, 128.1, 126.67, 126.64, 126.60, 126.58, 16.5, 15.7, −3.1. $^{29}Si\{^{1}H\}$ NMR (99 MHz): δ 7.9. Anal. Calcd for $C_{34}H_{34}S_4Si$: C, 68.18; H, 5.72. Found: C, 68.10; H, 5.67.

Preparation of 1,1-Dimethyl-2,5-bis[*p*-(*N*,*N*-dimethylamino)-phenyl]-3,4-diphenylsilole (3).[17b] The compound was prepared by a procedure similar to that for compound **1** above except for using 4-bromo-*N*,*N*-dimethylaniline (0.80 g, 4.0 mmol) as the cross-coupling reagent. The reaction mixture was quenched with 0.1 M NaOH and extracted with CH_2Cl_2 (2 × 30 mL), and the organics were combined and washed with water and brine and finally dried over magnesium sulfate. After filtration of the solution through a silica plug, the solvents were removed and the crude mixture was triturated with Et_2O to yield compound **3** as a bright yellow powder (0.50 g, 53% yield). ^{1}H NMR (500 MHz): δ 7.06−7.01 (m, 6H, ArH), 6.89−6.81 (m, 8H, ArH), 6.52−6.48 (m, 4H, ArH), 2.89 (s, 12 H, NMe), 0.51 (s, 6H, SiMe). $^{13}C\{^{1}H\}$ NMR (125 MHz): δ 151.8, 148.4, 140.5, 139.2, 130.3, 130.2, 128.0, 127.7, 125.9, 112.1, 40.5, −2.6.

Preparation of 1,1-Dimethyl-2,5-bis(2,2′-bipyridin-6-yl)-3,4-diphenylsilole (4).[19] The compound was prepared by a procedure similar to that for compound **1** above except for using 6-bromo-2,2′-bipyridine (0.47 g, 2.0 mmol) as the cross-coupling reagent and a smaller scale (1.0 mmol in dimethylbis(phenylethynyl)silane). The solvents of the reaction mixture were evaporated, and the crude material was subjected to silica gel column chromatography (hexanes/ethyl acetate 9/1). The eluted product was crystallized by slow evaporation from the eluting solvents to isolate compound **4** as a yellow crystalline material (0.22 g, 39%). ^{1}H NMR (500 MHz): δ 8.67 (ddd, *J* = 4.65, 1.83, 0.91 Hz, 2H, pyH), 8.42 (dt, *J* = 7.85, 1.36 Hz, 2H, pyH), 8.10 (dd, *J* = 7.85, 0.91 Hz, 2H, pyH), 7.85 (td, *J* = 7.85, 1.83 Hz, 2H, pyH), 7.39 (t, *J* = 7.85 Hz, 2H, pyH), 7.30 (ddd, *J* = 7.45, 4.67, 0.91 Hz, 2H, pyH), 7.17−7.14 (m, 6H, ArH), 7.00−6.97 (m, 4H, ArH), 6.58 (dd, *J* = 8.11, 0.86, 2H, ArH), 0.80 (s, 6H, SiMe). $^{13}C\{^{1}H\}$ NMR (125 MHz): δ 157.7, 156.9, 156.1, 155.4, 149.2, 144.3, 139.8, 137.0, 136.5, 129.4, 128.4, 126.9, 123.6, 123.2, 121.2, 118.1, −2.2.

Spectroscopy Studies with Metal Ions. Solutions of compounds **1**−**4** were prepared at a concentration of 1.0×10^{-4} M in spectrophotometric-grade methylene chloride. The metal perchlorate solutions were prepared in the following concentrations (equivalents) in spectrophotometric-grade methanol: 1.0×10^{-4} M (1 equiv), 2.0×10^{-4} M (2 equiv), 5.0×10^{-4} M (5 equiv), 1.0×10^{-3} M (10 equiv). The solutions were not degassed. To 2 mL of the silole solution in a quartz cuvette was added 2 mL of the above metal perchlorate solutions, and the solution was then analyzed by UV−visible and fluorescence spectroscopy.

X-ray Structure Determination of 1 and 2. Crystals of X-ray diffraction quality were grown by slow evaporation of an ether solution of **1** or by slow diffusion of methanol into a methylene chloride solution of **2**. Crystals with appropriate dimensions were mounted on a glass capillary in a random orientation. Preliminary examination and data collection were performed using a Bruker Kappa Apex II charge coupled device (CCD) detector system single-crystal X-ray diffractometer using an Oxford Cryostream LT device. Data were collected using graphite-monochromated Mo Kα radiation (λ = 0.71073 Å) from a fine focus sealed X-ray tube source. Preliminary unit cell constants were determined using a set of 36 narrow frame scans. Data sets consist of combinations of φ scan frames with a typical scan width of 0.5° and an exposure time of 15 s/frame at a crystal to detector distance of 4.0 cm. The collected frames were integrated using an orientation matrix determined from the narrow frame scans. Apex II and SAINT software packages were used for data collection and integration. Final cell constants were determined through global refinement of reflections from the complete data set. Systematic errors in the data were corrected using SADABS, on the basis of the Laue symmetry using equivalent reflections. Crystal data and intensity parameters are given in Table S-1 in the Supporting Information.

Structure solutions for **1** and **2** were carried out using SHELXS, and refinement was performed against the reduced data using SHELXL,[35] using the OLEX2 graphical interface software.[36] The structures were solved as orthorhombic unit cells by direct methods (**1**, *Pbca*; **2**, *Pbcn*) and refined with full matrix least-squares refinement by minimizing $\sum w(F_o^2 - F_c^2)^2$. All non-hydrogen atoms were refined to convergence. Compound **2** crystallized with three methylene chloride solvent molecules per molecule. One chlorine atom on one solvent molecule was disordered; this was addressed by refinement of the chlorine molecules over two positions at a ratio of 93/7 of their partial occupancies. Another methylene chloride molecule has a chlorine atom that was symmetrically generated, and the special position constraints were suppressed; the molecule also has a partial occupancy of 0.5. EADP constraints were employed on the chlorine atoms. The silicon atom in **2** is on a special position. All hydrogen atoms were added in the calculated positions and were refined using appropriate riding models. The models were refined to convergence to the final residual values of R_1 = 4.5% and wR_2 = 12.1% for **1** and R_1 = 6.1% and wR_2 = 14.3% for **2**. Complete listings of geometrical parameters, positional and isotropic displacement coefficients for hydrogen atoms, and anisotropic displacement coefficients for the non-hydrogen atoms are submitted as Supporting Information within the associated CIF files.

■ ASSOCIATED CONTENT

Ⓢ Supporting Information

CIF files and a table giving crystallographic data for with siloles **1** and **2** and figures giving UV−vis and fluorescence data for the siloles and all equivalents of each metal used, ^{1}H and ^{13}C{^{1}H} NMR spectra for siloles **1**−**4**, ^{29}Si{^{1}H} NMR spectra for the new siloles **1** and **2**, and a sketch of the proposed interaction of the metal cations with **3** and **4**. This material is available free of charge via the Internet at http://pubs.acs.org.

■ AUTHOR INFORMATION

Corresponding Author

*J.B.-W.: e-mail, wilkingj@umsl.edu; tel, 1-314-516-6436; fax, 1-314-516-5342.

Notes

The authors declare no competing financial interest.

■ ACKNOWLEDGMENTS

We thank Dr. Nigam P. Rath for his generous assistance in analyzing the crystallographic data and models. Funding from the National Science Foundation (MRI, CHE-0420497) for the Apex-II diffractometer is acknowledged and appreciated.

■ REFERENCES

(1) Murata, H.; Malliaras, G. G.; Uchida, M.; Shen, Y.; Kafafi, Z. H. *Chem. Phys. Lett.* **2001**, *339*, 161−166.

(2) Zhan, X.; Risko, C.; Amy, F.; Chan, C.; Zhao, W.; Barlow, S.; Kahn, A.; Brédas, J.-L.; Marder, S. R. *J. Am. Chem. Soc.* **2005**, *127*, 9021−9029.

(3) Yamaguchi, S.; Tamao, K. *Bull. Chem. Soc. Jpn.* **1996**, *69*, 2327−2334.

(4) Chen, J.; Law, C. C. W.; Lam, J. W. Y.; Dong, Y.; Lo, S. M. F.; Williams, I. D.; Zhu, D.; Tang, B. Z. *Chem. Mater.* **2003**, *15*, 1535−1546.

(5) Boydston, A. J.; Pagenkopf, B. L. *Angew. Chem.* **2004**, *116*, 6496−6498.

(6) Zhan, X.; Barlow, S.; Marder, S. R. *Chem. Commun.* **2009**, 1948−1955.

(7) Boydston, A. J.; Yin, Y.; Pagenkopf, B. L. *J. Am. Chem. Soc.* **2004**, *126*, 3724−3725.

(8) (a) Usta, H.; Lu, G.; Facchetti, A.; Marks, T. J. *J. Am. Chem. Soc.* **2006**, *128*, 9034−9035. (b) Wu, J.-S.; Cheng, Y.-J.; Lin, T.-Y.; Chang, C.-Y.; Shih, P.-I.; Hsu, C.-S. *Adv. Funct. Mater.* **2012**, *22*, 1711−1722. (c) Wang, Y.; Hou, L.; Yang, K.; Chen, J.; Wang, F.; Cao, Y. *Macromol. Chem. Phys.* **2005**, *206*, 2190−2198. (d) Huang, H.; Youn, J.; Ortiz, R. P.; Zheng, Y.; Facchetti, A.; Marks, T. *Chem. Mater.* **2011**, *23*, 2185−2200.

(9) (a) Murata, H.; Kafafi, Z. H. *Appl. Phys. Lett.* **2002**, *80*, 189−191. (b) Tamao, K.; Uchida, M.; Izumizawa, T.; Furukawa, K.; Yamaguchi, S. *J. Am. Chem. Soc.* **1996**, *118*, 11974−11975. (c) Kim, W.; Palilis, L. C.; Uchida, M.; Kafafi, Z. H. *Chem. Mater.* **2004**, *16*, 4681−4686.

(10) (a) Zhang, Z.-G.; Min, J.; Zhang, S.; Zhang, J.; Zhang, M.; Li, Y. *Chem. Commun.* **2011**, 9474−9476. (b) DiCarmine, P. M.; Wang, X.; Pagenkopf, B. L.; Semenikhin, O. A. *Electrochem. Commun.* **2008**, *10*, 229−232. (c) Hou, J.; Chen, H.-Y.; Zhang, S.; Li, G.; Yang, Y. *J. Am. Chem. Soc.* **2008**, *130*, 16144−16145. (d) Wang, F.; Luo, J.; Yang, K.; Chen, J.; Huang, F.; Cao, Y. *Macromolecules* **2005**, *38*, 2253−2260.

(11) (a) Li, Z.; Dong, Y. Q.; Lam, J. W. Y.; Sun, J.; Qin, A.; Häußler, M.; Dong, Y. P.; Sung, H. H. Y.; Williams, I. D.; Kwok, H. S.; Tang, B. Z. *Adv. Funct. Mater.* **2009**, *19*, 905−917. (b) Wang, M.; Zhang, D.; Zhang, G.; Tang, Y.; Wang, S.; Zhu, D. *Anal. Chem.* **2008**, *80*, 6443−6448. (c) Sohn, H.; Calhoun, R. M.; Sailor, M. J.; Trogler, W. C. *Angew. Chem., Int. Ed.* **2001**, *40*, 2104−2105.

(12) See for example: (a) McMahon, R. J. *Coord. Chem. Rev.* **1982**, *47*, 1−14. (b) Carré, F.; Colomer, E.; Corey, J. Y.; Corriu, R. J. P.; Guérin, C.; Henner, B. J. L.; Kolani, B.; Man, W.W.C.W.C. *Organometallics* **1986**, *5*, 910−917. (c) Ohshita, J.; Hamaguchi, T.; Toyoda, E.; Kunai, A.; Komaguchi, K.; Shiotani, M. *Organometallics* **1999**, *18*, 1717−1723. (d) Dysard, J. M.; Tilley, T. D. *J. Am. Chem. Soc.* **2000**, *122*, 3097−3105.

(13) Lee, J.; Liu, Q.-D.; Motala, M.; Dane, J.; Gao, J.; Kang, Y.; Wang, S. *Chem. Mater.* **2004**, *16*, 1869−1877.

(14) Aubouy, L.; Huby, N.; Wantz, G.; Vignau, L.; Hirsch, L.; Guérin, C.; Gerbier, P. *C. R. Chim.* **2005**, *8*, 1262−1267.

(15) Yin, S.; Zhang, J.; Feng, H.; Zhao, Z.; Xu, L.; Qiu, H.; Tang, B. Z. *Dyes Pigm.* **2012**, *95*, 174−179.

(16) (a) Braddock-Wilking, J.; Gao, L.-B.; Rath, N. P. *Organometallics* **2010**, *29*, 1612−1621. (b) Braddock-Wilking, J.; Gao, L.-B.; Rath, N. P. *Dalton Trans.* **2010**, *39*, 9321−9328.

(17) (a) Tamao, K.; Yamaguchi, S.; Shiro, M. *J. Am. Chem. Soc.* **1994**, *116*, 11715−11722. (b) Yamaguchi, S.; Endo, T.; Uchida, M.; Izumizawa, T.; Furukawa, K.; Tamao, K. *Chem. Eur. J.* **2000**, *6*, 1683−1692.

(18) Dötze, M.; Klar, G. *Phosphorus, Sulfur, Silicon Relat. Elem.* **1993**, *84*, 95−106.

(19) Uchida, M.; Izumizawa, T.; Nakano, T.; Yamaguchi, S.; Tamao, K.; Furukawa, K. *Chem. Mater.* **2001**, *13*, 2680−2683.

(20) Pagenkopf, B. L.; Morra, N. *Org. Synth.* **2008**, *85*, 53−63.

(21) Yu, G.; Yin, S.; Liu, Y.; Chen, J.; Xu, X.; Sun, X.; Ma, D.; Zhan, X.; Peng, Q.; Shuai, Z.; Tang, B. Z.; Zhu, D.; Fang, W.; Luo, Y. *J. Am. Chem. Soc.* **2005**, *127*, 6335−6346.

(22) Nishio, M. *Phys. Chem. Chem. Phys.* **2011**, *13*, 13873−13900.

(23) Son, H.-J.; Han, W.-S.; Wee, K. R.; Lee, S.-H.; Hwang, A.-R.; Kwon, S.; Cho, D. W.; Su, I.-H.; Kang, S. O. *J. Mater. Chem.* **2009**, *19*, 8964−8973.

(24) Mei, J.; Wang, J.; Sun, J. Z.; Zhao, H.; Yuan, W.; Deng, C.; Chen, S.; Sung, H. H. Y.; Lu, P.; Qin, A.; Kwok, H. S.; Ma, Y.; Williams, I. D.; Tang, B. Z. *Chem. Sci.* **2012**, *3*, 549−558.

(25) Linschitz, H.; Pekkarinen, L. *J. Am. Chem. Soc.* **1960**, *82*, 2411−2416.

(26) Nolan, E. M.; Lippard, S. J. *Chem. Rev.* **2008**, *108*, 3343−3380.

(27) Berlman, I. B. *J. Phys. Chem.* **1973**, *77*, 562−567.

(28) Rurack, K. *Spectrochim. Acta, Part A* **2001**, *57*, 2161−2195. Relevant information is contained in section 4.1.2.

(29) Behrens, U.; Berges, P.; Bieganowski, R.; Hinrichs, W.; Schiffling, C.; Klar, G. *J. Chem. Res., Synop.* **1986**, *9*, 326−327.

(30) Pearson, R. G. *J. Am. Chem. Soc.* **1963**, *85*, 3533−3539.

(31) Valeur, B.; Leray, I. *Coord. Chem. Rev.* **2000**, *205*, 3−40. Relevant information on PCT is contained in section 3.

(32) Helm, H.; Merbach, A. E. *Chem. Rev.* **2005**, *105*, 1923−1959.

(33) Boag, N. M. Transition Metal Catalysis. In *Inorganic Experiments*, 3rd ed.; Woolins, J. D., Ed.; Wiley-VCH: Weinheim, Germany, 2010; p 205.

(34) Chau, N. T. T.; Meyer, M.; Komagawa, S.; Chevallier, F.; Fort, Y.; Uchiyama, M.; Mongin, F.; Gros, P. C. *Chem. Eur. J.* **2010**, *16*, 12425−12433.

(35) Sheldrick, G. M. *Acta Crystallogr.* **2008**, *A64*, 112−122.

(36) Dolomanov, O. V.; Bourhis, L. J.; Gildea, R. J.; Howard, J. A. K.; Puschmann, H. *J. Appl. Crystallogr.* **2009**, *42*, 339−341.